RESEARCH ARTICLE SUMMARY

CLINICAL TRIALS

CRISPR-engineered T cells in patients with refractory cancer

Edward A. Stadtmauer*†, Joseph A. Fraietta*, Megan M. Davis, Adam D. Cohen, Kristy L. Weber, Eric Lancaster, Patricia A. Mangan, Irina Kulikovskaya, Minnal Gupta, Fang Chen, Lifeng Tian, Vanessa E. Gonzalez, Jun Xu, In-young Jung, J. Joseph Melenhorst, Gabriela Plesa, Joanne Shea, Tina Matlawski, Amanda Cervini, Avery L. Gaymon, Stephanie Desjardins, Anne Lamontagne, January Salas-Mckee, Andrew Fesnak, Donald L. Siegel, Bruce L. Levine, Julie K. Jadlowsky, Regina M. Young, Anne Chew, Wei-Ting Hwang, Elizabeth O. Hexner, Beatriz M. Carreno, Christopher L. Nobles, Frederic D. Bushman, Kevin R. Parker, Yanyan Qi, Ansuman T. Satpathy, Howard Y. Chang, Yangbing Zhao, Simon F. Lacey*, Carl H. June*†

INTRODUCTION: Most cancers are recognized and attacked by the immune system but can progress owing to tumor-mediated immunosuppression and immune evasion mechanisms. The infusion of ex vivo engineered T cells, termed adoptive T cell therapy, can increase the natural antitumor immune response of the patient. Gene therapy to redirect immune specificity combined with genome editing has the potential to improve the efficacy and increase the safety of engineered T cells. CRISPR coupled with CRISPR-associated protein 9 (Cas9) endonuclease is a powerful gene-editing technology that potentially allows the ability to target multiple genes in T cells to improve cancer immunotherapy.

RATIONALE: Our first-in-human, phase 1 clinical trial (clinicaltrials.gov; trial NCT03399448) was designed to test the safety and feasibility of multiplex CRISPR-Cas9 gene editing of T cells from patients with advanced, refractory cancer. A limitation of adoptively transferred T cell efficacy has been the induction of T cell dysfunction or exhaustion. We hypothesized that removing the endogenous T cell receptor (TCR) and the immune checkpoint molecule programmed cell death protein 1 (PD-1) would improve the function and persistence of engineered T cells. In addition, the removal of PD-1 has the potential to improve safety and reduce toxicity that can be caused by autoimmunity.

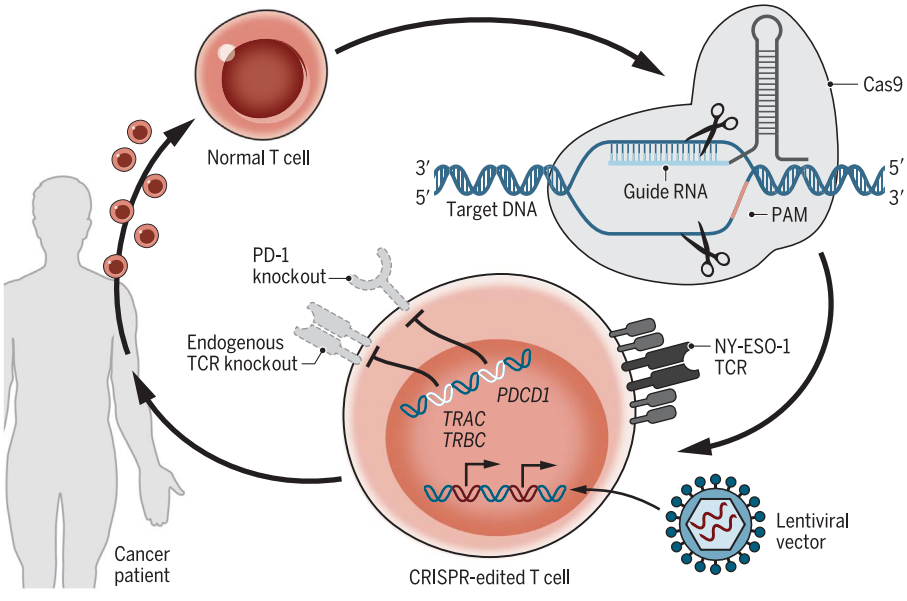

CRISPR-Cas9 engineering of T cells in cancer patients. T cells (center) were isolated from the blood of a patient with cancer. CRISPR-Cas9 ribonuclear protein complexes loaded with three sgRNAs were electroporated into the normal T cells, resulting in gene editing of the *TRAC*, *TRBC1*, *TRBC2*, and *PDCD1* (encoding PD-1) loci. The cells were then transduced with a lentiviral vector to express a TCR specific for the cancer-testis antigens NY-ESO-1 and LAGE-1 (right). The engineered T cells were then returned to the patient by intravenous infusion, and patients were monitored to determine safety and feasibility. PAM, protospacer adjacent motif.

A synthetic, cancer-specific TCR transgene (NY-ESO-1) was also introduced to recognize tumor cells. In vivo tracking and persistence of the engineered T cells were monitored to determine if the cells could persist after CRISPR-Cas9 modifications.

RESULTS: Four cell products were manufactured at clinical scale, and three patients (two with advanced refractory myeloma and one with metastatic sarcoma) were infused. The editing efficiency was consistent in all four products and varied as a function of the single guide RNA (sgRNA), with highest efficiency observed for the TCR α chain gene (*TRAC*) and lowest efficiency for the TCR β chain gene (*TRBC*). The mutations induced by CRISPR-Cas9 were highly specific for the targeted loci; however, rare off-target edits were observed. Single-cell RNA sequencing of the infused CRISPR-engineered T cells revealed that ~30% of cells had no detectable mutations, whereas ~40% had a single mutation and ~20 and ~10% of the engineered T cells were double mutated and triple mutated, respectively, at the target sequences. The edited T cells engrafted in all three patients at stable levels for at least 9 months. The persistence of the T cells expressing the engineered TCR was much more durable than in three previous clinical trials during which T cells were infused that retained expression of the endogenous TCR and endogenous PD-1. There were no clinical toxicities associated with the engineered T cells. Chromosomal translocations were observed in vitro during cell manufacturing, and these decreased over time after infusion into patients. Biopsies of bone marrow and tumor showed trafficking of T cells to the sites of tumor in all three patients. Although tumor biopsies revealed residual tumor, in both patients with myeloma, there was a reduction in the target antigens NY-ESO-1 and/or LAGE-1. This result is consistent with an on-target effect of the engineered T cells, resulting in tumor evasion.

ON OUR WEBSITE

Read the full article at http://dx.doi.org/10.1126/science.aba7365

CONCLUSION: Preliminary results from this pilot trial demonstrate that multiplex human genome engineering is safe and feasible using CRISPR-Cas9. The extended persistence of the engineered T cells indicates that preexisting immune responses to Cas9 do not appear to present a barrier to the implementation of this promising technology. ■

The list of author affiliations is available in the full article online.
*These authors contributed equally to this work.
†Corresponding author. Email: edward.stadtmauer@pennmedicine.upenn.edu (E.A.S.); cjune@upenn.edu (C.H.J.)
Cite this article as E. A. Stadtmauer *et al.*, *Science* **367**, eaba7365 (2020). DOI: 10.1126/science.aba7365

RESEARCH ARTICLE

CLINICAL TRIALS

CRISPR-engineered T cells in patients with refractory cancer

Edward A. Stadtmauer[1,2]*†, Joseph A. Fraietta[2,3,4,5,6]*, Megan M. Davis[5,6], Adam D. Cohen[1,2], Kristy L. Weber[2,7], Eric Lancaster[8], Patricia A. Mangan[1], Irina Kulikovskaya[5], Minnal Gupta[5], Fang Chen[5], Lifeng Tian[5], Vanessa E. Gonzalez[5], Jun Xu[5], In-young Jung[4,5], J. Joseph Melenhorst[3,5,6], Gabriela Plesa[5], Joanne Shea[5], Tina Matlawski[5], Amanda Cervini[5], Avery L. Gaymon[5], Stephanie Desjardins[5], Anne Lamontagne[5], January Salas-Mckee[5], Andrew Fesnak[5,6], Donald L. Siegel[5,6], Bruce L. Levine[5,6], Julie K. Jadlowsky[5], Regina M. Young[5], Anne Chew[5], Wei-Ting Hwang[9], Elizabeth O. Hexner[1,2], Beatriz M. Carreno[3,5,6], Christopher L. Nobles[4], Frederic D. Bushman[4], Kevin R. Parker[10], Yanyan Qi[11], Ansuman T. Satpathy[10,11], Howard Y. Chang[10,12], Yangbing Zhao[5,6], Simon F. Lacey[5,6]*, Carl H. June[2,3,5,6]*†

CRISPR-Cas9 gene editing provides a powerful tool to enhance the natural ability of human T cells to fight cancer. We report a first-in-human phase 1 clinical trial to test the safety and feasibility of multiplex CRISPR-Cas9 editing to engineer T cells in three patients with refractory cancer. Two genes encoding the endogenous T cell receptor (TCR) chains, TCRα (*TRAC*) and TCRβ (*TRBC*), were deleted in T cells to reduce TCR mispairing and to enhance the expression of a synthetic, cancer-specific TCR transgene (NY-ESO-1). Removal of a third gene encoding programmed cell death protein 1 (PD-1; *PDCD1*), was performed to improve antitumor immunity. Adoptive transfer of engineered T cells into patients resulted in durable engraftment with edits at all three genomic loci. Although chromosomal translocations were detected, the frequency decreased over time. Modified T cells persisted for up to 9 months, suggesting that immunogenicity is minimal under these conditions and demonstrating the feasibility of CRISPR gene editing for cancer immunotherapy.

Gene editing offers the potential to correct DNA mutations and may offer promise to treat or eliminate countless human genetic diseases. The goal of gene editing is to change the DNA of cells with single–base pair precision. The principle was first demonstrated in mammalian cells when it was shown that expression of a rare cutting endonuclease to create double-strand DNA breaks resulted in repair by homologous and nonhomologous recombination (*1*). A variety of engineered nucleases were then developed to increase efficiency and enable potential therapeutic applications, including zinc finger nucleases, homing endonucleases, transcription activator–like effector nucleases, and CRISPR-Cas9 (clustered regularly interspaced short palindromic repeats associated with Cas9 endonuclease) (*2*). The first pilot human trials using genome editing were conducted in patients with HIV/AIDS and targeted the white blood cell protein CCR5, with the goal of mutating the *CCR5* gene by nonhomologous recombination and thereby inducing resistance to HIV infection (*3*, *4*). The incorporation of multiple guide sequences in CRISPR-Cas9 permits, in principle, multiplex genome engineering at several sites within a mammalian genome (*5*–*9*). The ability of CRISPR to facilitate efficient multiplex genome editing has greatly expanded the scope of possible targeted genetic manipulations, enabling new possibilities such as simultaneous deletion or insertion of multiple DNA sequences in a single round of mutagenesis. The prospect of using CRISPR engineering to treat a host of diseases, such as inherited blood disorders and blindness, is moving closer to reality.

Recent advances in CRISPR-Cas9 technology have also permitted efficient DNA modifications in human T cells, which holds great promise for enhancing the efficacy of cancer therapy. T lymphocytes are specialized immune cells that are largely at the core of the modern-day cancer immunotherapy revolution. The T cell receptor (TCR) complex is located on the surface of T cells and is central for initiating successful antitumor responses by recognizing foreign antigens and peptides bound to major histocompatibility complex molecules. One of the most promising areas of cancer immunotherapy involves adoptive cell therapy, whereby the patient's own T cells are genetically engineered to express a synthetic (transgenic) TCR that can specifically detect and kill tumor cells. Recent studies have shown safety and promising efficacy of such adoptive T cell transfer approaches using transgenic TCRs specific for the immunogenic NY-ESO-1 tumor antigen in patients with myeloma, melanoma, and sarcoma (*10*–*12*). One limitation of this approach is that the transgenic TCR has been shown to mispair and/or compete for expression with the α and β chains of the endogenous TCR (*13*–*15*). Mispairing of the therapeutic TCR α and β chains with endogenous α and β chains reduces therapeutic TCR cell surface expression and potentially generates self-reactive TCRs.

A further shortcoming of adoptively transferred T cells has been the induction of T cell dysfunction or exhaustion leading to reduced efficacy (*16*). Programmed cell death protein 1 (PD-1)–deficient allogeneic mouse T cells with transgenic TCRs showed enhanced responses to alloantigens, indicating that the PD-1 protein on T cells plays a negative regulatory role in antigen responses that are likely to be cell intrinsic (*17*). The adoptive transfer of PD-1–deficient T cells in mice with chronic lymphocytic choriomeningitis virus infection initially leads to enhanced cytotoxicity and later to enhanced accumulation of terminally differentiated T cells (*18*). Antibody blockade of PD-1, or disruption or knockdown of the gene encoding PD-1 (i.e., *PDCD1*), improved chimeric antigen receptor (CAR) or TCR T cell–mediated killing of tumor cells in vitro and enhanced clearance of PD-1 ligand–positive (PD-L1$^+$) tumor xenografts in vivo (*19*–*23*). In preclinical studies, we and others found that CRISPR-Cas9–mediated disruption of *PDCD1* in human T cells transduced with a CAR increased antitumor efficacy in tumor xenografts (*24*–*26*). Adoptive transfer of transgenic TCR T cells specific for the cancer antigen NY-ESO-1, in combination with a monoclonal antibody targeting PD-1, enhanced antitumor efficacy in mice (*27*). We therefore designed a first-in-human, phase 1 human clinical trial to test the safety and feasibility of multiplex CRISPR-Cas9 genome editing for a synthetic biology cancer immunotherapy application. We chose to target endogenous *TRAC*, *TRBC*, and *PDCD1*

[1]Division of Hematology-Oncology, Department of Medicine, Perelman School of Medicine, University of Pennsylvania, Philadelphia, PA, USA. [2]Abramson Cancer Center, Perelman School of Medicine, University of Pennsylvania, Philadelphia, PA, USA. [3]Parker Institute for Cancer Immunotherapy, Perelman School of Medicine, University of Pennsylvania, Philadelphia, PA, USA. [4]Department of Microbiology, Perelman School of Medicine, University of Pennsylvania, Philadelphia, PA, USA. [5]Center for Cellular Immunotherapies, Perelman School of Medicine, University of Pennsylvania, Philadelphia, PA, USA. [6]Department of Pathology and Laboratory Medicine, Perelman School of Medicine, University of Pennsylvania, Philadelphia, PA, USA. [7]Department of Orthopaedic Surgery, Perelman School of Medicine, University of Pennsylvania, Philadelphia, PA, USA. [8]Department of Neurology, Perelman School of Medicine, University of Pennsylvania, Philadelphia, PA, USA. [9]Department of Biostatistics, Epidemiology and Informatics, Perelman School of Medicine, University of Pennsylvania, Philadelphia, PA, USA. [10]Center for Personal Dynamic Regulomes, Stanford University School of Medicine, Stanford, CA, USA. [11]Department of Pathology, Stanford University School of Medicine, Stanford, CA, USA. [12]Howard Hughes Medical Institute, Stanford University School of Medicine, Stanford, CA, USA.
*These authors contributed equally to this work.
†Corresponding author. Email: edward.stadtmauer@pennmedicine.upenn.edu (E.A.S.); cjune@upenn.edu (C.H.J.)

on T cells to increase the safety and efficacy profile of NY-ESO-1 TCR–expressing engineered cells. In principle, this strategy allowed us to increase exogenous TCR expression and reduce the potential for mixed heterodimer formation (i.e., by deleting the α and β TCR domain genes *TRAC* and *TRBC*, respectively) and to limit the development of T cell exhaustion, which can be triggered by the checkpoint ligands PD-L1 and PD-L2 (i.e., by deleting *PDCD1*).

Results

Clinical protocol

The phase 1 human trial (clinicaltrials.gov; trial NCT03399448) was designed to assess the safety and feasibility of infusing autologous NY-ESO-1 TCR–engineered T cells in patients after CRISPR-Cas9 editing of the *TRAC*, *TRBC*, and *PDCD1* loci. During the manufacturing process, cells were taken out of the cancer patient, engineered, and then infused back into the individual. The genetically engineered T cell product was termed "NYCE" (NY-ESO-1–transduced CRISPR 3X edited cells) and is referred to as NYCE hereafter. During clinical development of the protocol, we elected to use a TCR rather than a CAR because the incidence of cytokine release syndrome is generally less prevalent using TCRs (*11*). In principle, this allowed a more discriminating assessment of whether gene editing with Cas9 was potentially immunogenic or toxic when compared with the baseline low level of adverse events observed in our previous clinical trial targeting NY-ESO-1 with transgenic TCRs (*11*). The autologous T cells were engineered by lentiviral transduction to express an HLA-A2*0201–restricted TCR specific for the SLLMWITQC peptide in NY-ESO-1 and LAGE-1. The manufacturing process, vector design, and clinical protocol for NYCE T cells are described in the materials and methods and are depicted schematically (figs. S1 and S2). Of the six patients who were initially enrolled, four patients had successfully engineered T cells that were subjected to detailed release criteria testing as specified in the U.S. Food and Drug Administration (FDA)–accepted Investigational New Drug application (table S1) (see fig. S3 for the consort diagram). Of the four patients with cell products available, one patient assigned unique patient number (UPN) 27 experienced rapid clinical progression and was no longer eligible for infusion owing to the inability to meet protocol-mandated safety criteria (see supplementary materials). Of the three patients who were infused with CRISPR-Cas9–engineered T cells, two patients had refractory advanced myeloma and one patient had a refractory metastatic sarcoma not responding to multiple prior therapies (Table 1). The patients were given lymphodepleting chemotherapy with cyclophosphamide and fludarabine on days −5 to −3 (i.e., before administration with CRISPR-Cas9–engineered T cells) and a single infusion of 1×10^8 manufactured CRISPR-Cas9–engineered T cells per kilogram on day 0 of the protocol (fig. S2). No cytokines were administered to the patients.

Characteristics of infused CRISPR-Cas9–engineered T cell products

The T cell product was manufactured by electroporation of ribonucleoprotein complexes (RNPs) comprising recombinant Cas9 loaded with equimolar mixtures of single guide RNA (sgRNA) for *TRAC*, *TRBC*, and *PDCD1* followed by lentiviral transduction of the transgenic TCR (Fig. 1A). All products were expanded to $>1 \times 10^{10}$ T cells by the time of harvest (Fig. 1B). The transgenic TCR could be detected by

Table 1. Patient demographics and date of engineered T cell infusion. MM, multiple myeloma; BM, bone marrow; XRT, radiation therapy; ASCT, autologous hematopoietic stem cell transplant; ND, not done.

Subject ID (UPN) and infusion date	Sex and age	Diagnosis	Clinical sites	Prior therapy	Prior transplant or surgery	LAGE-1*, NY-ESO-1*, NY-ESO-1**
UPN35 7 January 2019	Female 66 years	Immunoglobulin G kappa MM 2008	BM, lytic bone lesions	Lenalidomide, pomalidomide, bortezomib, carfilzomib, daratumumab, panobinostat, etc. (eight lines of therapy; see supplementary materials)	Three ASCTs	Positive, positive, negative
UPN39 18 March 2019	Male 66 years	Myxoid and round cell liposarcoma 2012	Abdominal and pelvic masses	Doxorubicin, ifosfamide, XRT 60 gray, trabectedin, gemcitabine, taxol, XRT	Resection and debulking twice, left nephrectomy and partial sigmoid resection	ND, ND, positive
UPN07 5 August 2019	Female 62 years	Kappa light chain MM 2009	BM, lytic bone lesions	Lenalidomide, pomalidomide, bortezomib, carfilzomib, daratumumab, anti-CD38 immunoconjugate (six lines of therapy; see supplementary materials)	Two ASCTs	Positive, positive, negative

*qPCR **Immunohistochemistry

flow cytometric staining for Vβ8.1 or dextramer staining, ranging from 2 to 7% of T cells in the final product (Fig. 1C). The frequency of editing, as determined by digital polymerase chain reaction (PCR), varied according to the sgRNA and was about 45% for *TRAC*, 15% for *TRBC*, and 20% for *PDCD1* (Fig. 1D). Final product transduction efficiency, CD4:CD8 ratio, and dosing are shown in table S2.

The potency of the final engineered T cells was assessed by coculture with HLA-A2$^+$ tumor cells engineered to express NY-ESO-1 (Fig. 2A). The engineered T cells had potent antigen-specific cytotoxicity over a wide range of effector-to–target cell ratios. Interestingly, the cells treated with CRISPR-Cas9 were more cytotoxic than control cells transduced with the TCR but electroporated without CRISPR-Cas9 (i.e., cells that retained endogenous TCR). This is consistent with previous findings in mouse T cells, when a transgenic TCR was inserted into the endogenous locus, ablating expression of the endogenous TCR (*15*). Further studies will be required to determine if PD-1 knockout contributes to the increased potency afforded by knockout of the endogenous TCR.

We developed a sensitive immunoassay for detection of *Streptococcus pyogenes* Cas9 protein and quantified Cas9 early in the manufacturing process, showing declining levels that were <0.75 fg per cell in the harvested final product (Fig. 2C). Using a competitive fluorescence enzyme-linked immunosorbent assay (ELISA) screen, we found that healthy donors have humoral reactivity to Cas9 in serum (data not shown) and T cells (Fig. 2E), confirming previous reports (*28*–*30*). Interestingly, we found that the three patients tested at a variety of time points after infusion of the engineered T cells did not develop humoral responses to Cas9. The lack of immunization to Cas9 is consistent with the extended persistence of the infused cells (Fig. 3) and could be a consequence of the low content of Cas9 in the infused product and/or to the immunodeficiency in the patients as a result of their extensive previous treatment histories (Table 1).

Engraftment and persistence of infused CRISPR-Cas9–engineered T cells in cancer patients

Three patients with advanced, refractory cancer were given infusions of the CRISPR-Cas9–engineered T cells. The infusions were well tolerated, with no serious adverse events (Table 2); importantly, there were no cases of cytokine release syndrome, which is a potentially life-threatening systemic inflammatory response that has been associated with cancer immunotherapies (*31*). All three patients

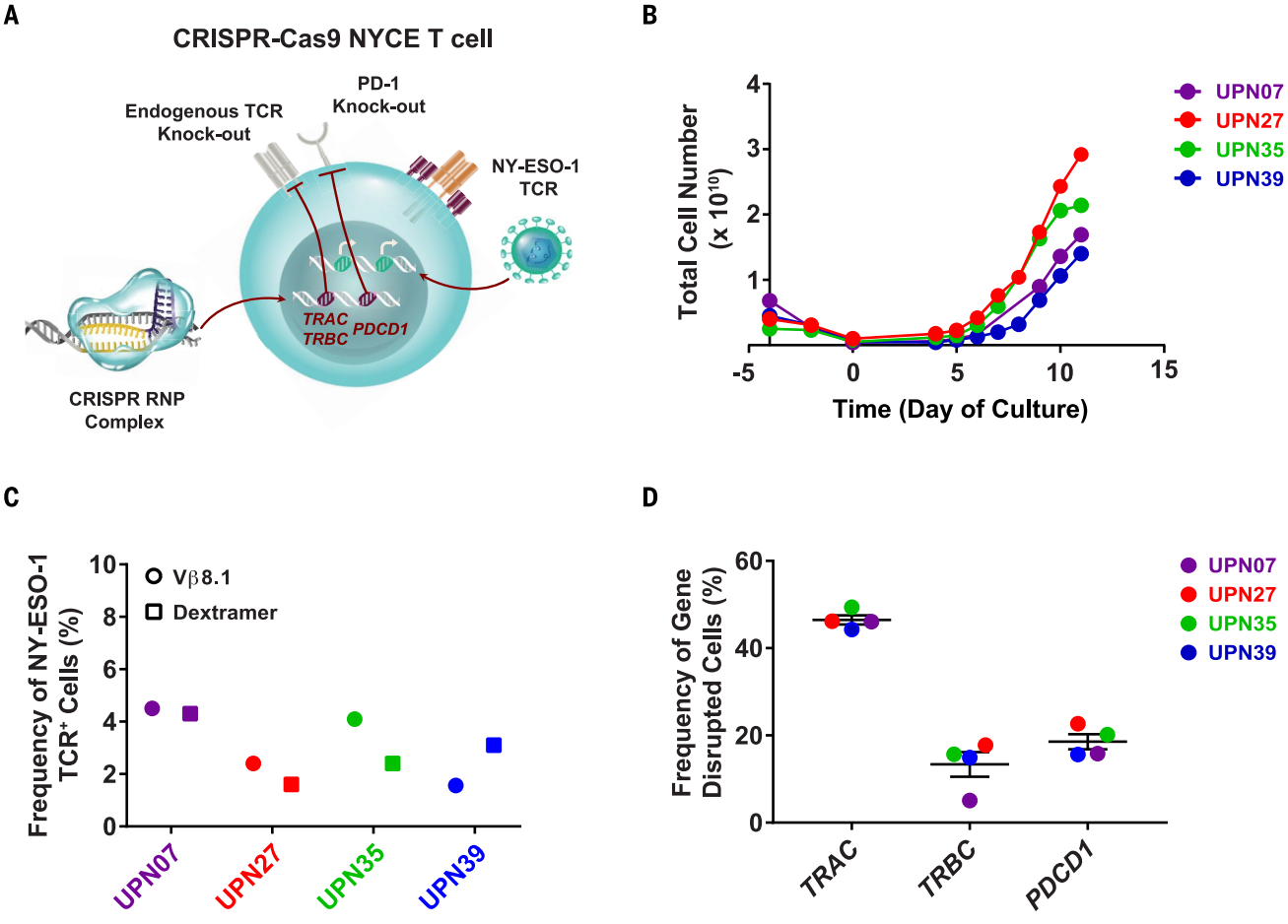

Fig. 1. Feasibility of CRISPR-Cas9 NYCE T cell engineering. (**A**) Schematic representation of CRISPR-Cas9 NYCE T cells. (**B**) Large-scale expansion of NYCE T cells. Autologous T cells were transfected with Cas9 protein complexed with sgRNAs (RNP complex) against *TRAC*, *TRBC* (i.e., endogenous TCR deletion), and *PDCD1* (i.e., PD-1 deletion) and subsequently transduced with a lentiviral vector to express a transgenic NY-ESO-1 cancer-specific TCR. Cells were expanded in dynamic culture for 8 to 12 days. On the final day of culture, NYCE T cells were harvested and cryopreserved in infusible medium. The total number of enriched T cells during culture is plotted for all four subjects (UPN07, UPN27, UPN35, and UPN39). (**C**) NY-ESO-1 TCR transduction efficiency was determined in harvested infusion products by flow cytometry. Data are gated on live CD3-expressing and Vβ8.1- or dextramer-positive lymphocytes and further gated on CD4-positive and/or CD8-positive cells. (**D**) The frequencies of *TRAC*, *TRBC*, and *PDCD1* gene-disrupted total cells in NYCE infusion products were measured using chip-based digital PCR. All data are representative of at least two independent experiments. Error bars represent mean ± SEM.

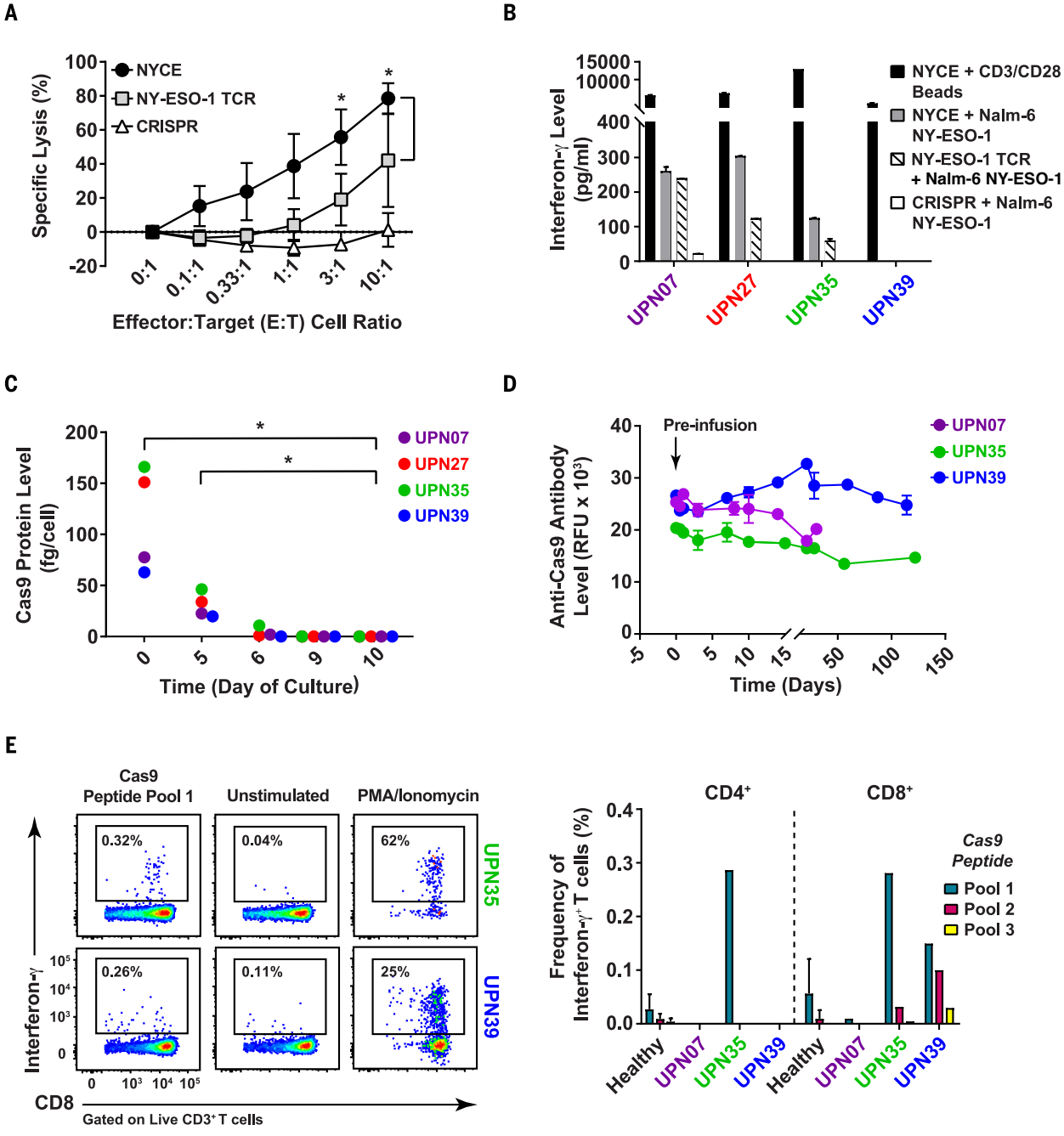

Fig. 2. Potency and immunogenicity of CRISPR-Cas9 engineered T cells. (**A**) Cytotoxicity of NYCE T cells cocultured with HLA-A*0201–positive Nalm-6 tumor cells engineered to express NY-ESO-1 and luciferase. Patient T cells transduced with the NY-ESO-1 TCR without CRISPR-Cas9 editing (NY-ESO-1 TCR) and untransduced T cells with CRISPR-Cas9 editing of *TRAC*, *TRBC*, and *PDCD1* (labeled CRISPR) were included as controls (n = 4 patient T cell infusion products). Asterisks indicate statistical significance determined by paired Student's t tests between groups (*P < 0.05). Error bars represent SEM. (**B**) Levels of soluble interferon-γ produced by patient NYCE T cell infusion products (labeled NYCE) after a 24-hour coculture with anti-CD3 and anti-CD28 antibody-coated beads or NY-ESO-1–expressing Nalm-6 target cells. Patient NY-ESO-1 TCR–transduced T cells (NY-ESO-1 TCR) and untransduced, CRISPR-Cas9–edited T cells (labeled CRISPR) served as controls. Error bars represent SEM. (**C**) Quantification of residual Cas9 protein in NYCE T cell infusion products in clinical-scale manufacturing is shown over time. Asterisks indicate statistical significance determined by paired Student's t tests between time points (*P < 0.05). (**D**) Results from the fluorescence-based indirect ELISA screen performed to detect antibodies against Cas9 protein in the sera of three patients treated with NYCE T cells. Each dot represents the amount of anti-Cas9 signals detected in patient serum before T cell infusion (indicated by a vertical black arrow) and at various time points after NYCE T cell transfer. RFU, relative fluorescent units. (**E**) Immunoreactive Cas9-specific T cells in baseline patient leukapheresis samples were detected. Representative flow cytometry plots (left) from two patients whose T cells were positive for interferon-γ in response to Cas9 peptide stimulation. Unstimulated T cells treated with vehicle alone (dimethyl sulfoxide, DMSO) served as a negative control, whereas matched T cells stimulated with phorbol myristate acetate (PMA) and ionomycin served as a positive control. Bar graphs (right) show the frequency of ex vivo CD4⁺ and CD8⁺ T cells from patients or healthy donor controls (n = 6) that secrete interferon-γ in response to stimulation with three different Cas9 peptide pools. The background frequency of interferon-γ–expressing T cells (unstimulated control group, DMSO alone) is subtracted from the values shown in the bar graph. Error bars represent SD.

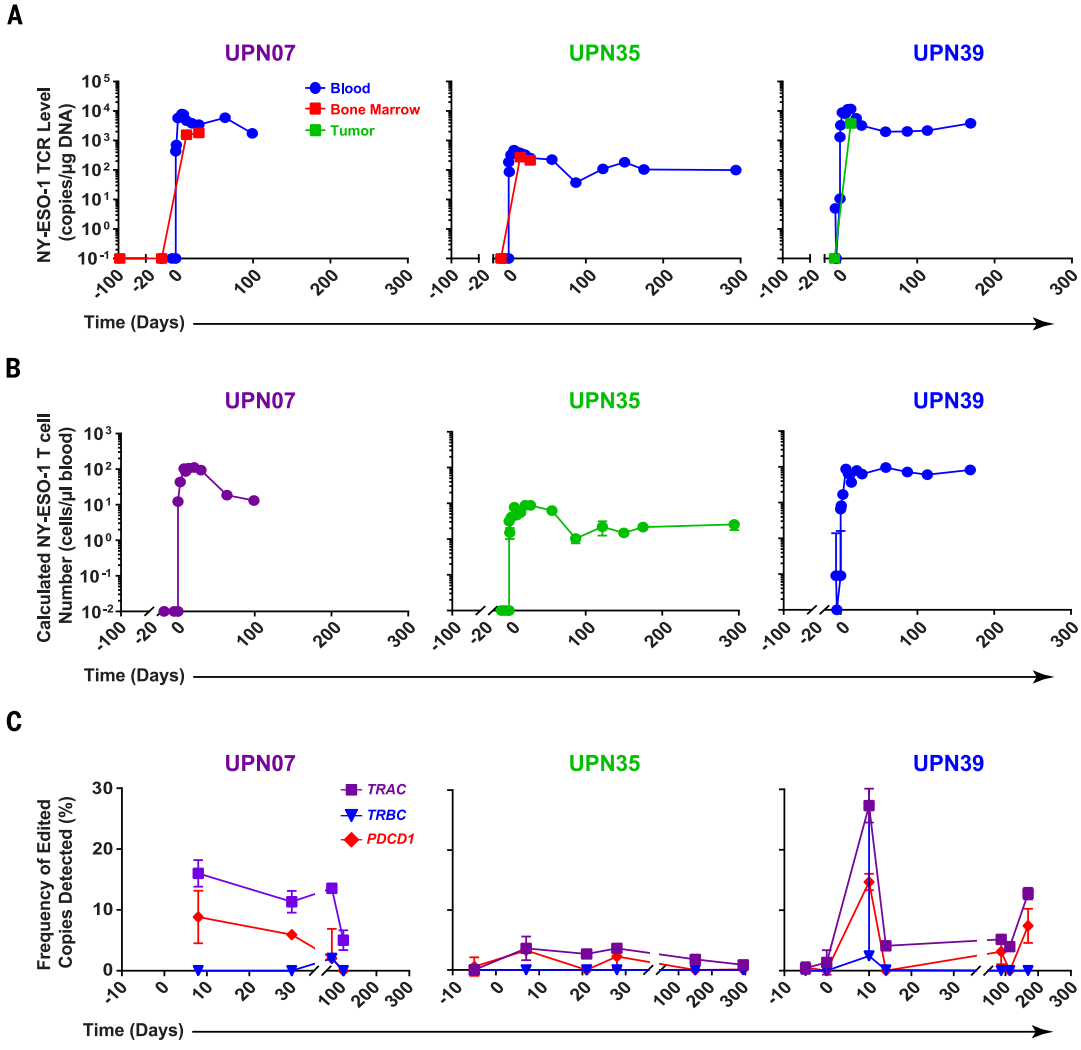

Fig. 3. Sustained in vivo expansion and persistence of CRISPR-Cas9–engineered T cells in patients. (**A**) The total number of vector copies per microgram of genomic DNA of the NY-ESO-1 TCR transgene in the peripheral blood (UPN07, UPN35, and UPN39), bone marrow (UPN07 and UPN35; multiple myeloma), and tumor (UPN39; sarcoma) is shown pre– and post–NYCE T cell infusion. (**B**) Calculated absolute numbers of NY-ESO-1 TCR–expressing T cells per microliter of whole blood from the time of infusion to various postinfusion time points in the study are shown. The limit of detection is about 2.5 cells per microliter of whole blood. (**C**) Frequencies of CRISPR-Cas9–edited T cells (*TRAC*, *TRBC*, and *PDCD1* knockout) before and after adoptive cell transfer are depicted. Error bars represent SD.

were infused with 1×10^8 cells/kg, and, owing to the considerable variation in TCR transduction efficiencies (table S2), the absolute number of infused engineered T cells ranged from 6.0×10^7 to 7.1×10^8 cells. Despite the variation in engineered cells, there were high peak levels and sustained persistence of the engineered cells in the blood of all three patients (Fig. 3A). The peak and steady-state levels of engineered cells were lowest in patient UPN35, who also had the lowest transduction efficiency (table S2). The persistence of the transduced cells is notably stable from 3 to 9 months after infusion, varying from 5 to 50 cells per microliter of blood (Fig. 3B). Using a subject-specific piecewise linear model, the decay half-lives of the transduced cells were 20.3, 121.8, and 293.5 days for UPN07, UPN35, and UPN39, respectively. The average decay half-life was 83.9 days (15 to 153 days, 95% confidence interval) for the three subjects, as estimated by a piecewise linear mixed-effects model that assumes cells decay linearly from day 14 postexpansion and random effects to allow varying level of expansion (or peak values) across subjects. The stable engraftment of our engineered T cells is notably different from previously reported trials with NY-ESO-1 TCR–engineered T cells, in which the half-life of the cells in blood was ~1 week (*11*, *32*, *33*). Biopsy specimens of bone marrow in the myeloma patients and tumor in the sarcoma patient demonstrated trafficking of the engineered T cells to the tumor in all three patients at levels approaching those in the blood compartment (Fig. 3A).

To determine the engraftment frequency of the CRISPR-Cas9 gene-edited cells, we initially used chip-based digital PCR. With this assay, engraftment of cells with editing at the *TRAC* and *PDCD1* loci was evident in all three patients (Fig. 3C). There was sustained persistence of *TRAC* and *PDCD1* edits in patients UPN39 and UPN07 at frequencies of 5 to 10% of circulating peripheral blood mononuclear cells (PBMCs), whereas *TRBC*-edited cells were lowest in frequency and only transiently detected. The low-level engraftment of *TRBC*-edited cells is likely related to the observation that this locus had the lowest level of editing efficiency in our preclinical studies (*25*) and in the harvested products (Fig. 1D).

Analysis of the fidelity of CRISPR-Cas9 genome editing

On- and off-target editing efficiency was assessed in the NYCE cells at the end of product manufacturing. Details of the analysis for UPN07 are shown as an example in Fig. 4, with detailed analysis of the other three manufactured products shown in table S3. The average on-target CRISPR-Cas9 editing efficiency for all engineered T cell products for each target is shown in Table 3. We used iGUIDE (*34*), a modification of the GUIDE sequencing (GUIDE-seq) method (*35*), to analyze the Cas9-mediated cleavage specificity. A complication of assays to assess repair by nonhomologous end joining (NHEJ) is that DNA double-strand breaks are formed spontaneously during cell division at high rates in the absence of added nucleases (*36*), which can

Table 2. List of adverse events in the study. "–" indicates no adverse event.

Adverse events category	Toxicity	All grades	Grade 1 or 2	Grade 3 or 4
Hematologic	Anemia	2	1	1
	Leukopenia	4	–	4
	Neutropenia	4	1	3
	Thrombocytopenia	6	3	3
	Lymphopenia	1	–	1
Infection	Upper respiratory	1	1	–
	Febrile neutropenia	2	–	2
Electrolyte	Hypercalcemia	1	1	–
	Hyperphosphatemia	1	1	–
	Hypoalbuminemia	1	1	–
	Hypocalcemia	3	2	1
	Hypokalemia	1	1	–
	Hypomagnesemia	1	1	–
	Hyponatremia	1	1	–
	Hypophosphatemia	1	–	1
Neurologic	Dysgeusia	1	1	–
	Headache	1	1	–
	Paresthesia	2	2	–
	Syncope	1	–	1
	Pain	3	3	–
Renal	Acute kidney injury	1	1	–
	Urinary obstruction	1	–	1
Respiratory	Aspiration	1	–	1
	Nasal congestion	1	1	–
	Cough	2	2	–
Gastrointestinal	Lower gastrointestinal bleed	1	1	–
	Vomiting	1	1	–
Other	Alopecia	1	1	–
	Phlebitis	1	1	–
	Lower-extremity edema	1	1	–
Total		50	30	20

increase the background in assays of off-target cleavage. The distribution of on- and off-target cleavage is expected to vary for the three sgRNAs that were used in the manufacturing process (fig. S1A). Of the three sgRNAs, there were more off-target mutations identified for *TRBC* than for the other loci (Fig. 4C and figs. S4 and S5). The sgRNA for *PDCD1* was the most specific, because very few off-target edits were identified in more than 7000 sites of cleavage and there were very few off-target reads identified at the *TRAC1* and *TRAC2* loci (Fig. 4C).

The genomic localization of identified DNA cleavage sites was as expected, given the chromosomal location of the three targeted genes on chromosomes 2, 7, and 14 (Fig. 4A). The distribution of the incorporation of the double-stranded oligodeoxynucleotide (dsODN) label around on-target sites, based on pileups within a window of 100 base pairs (bp), is shown in Fig. 4B and fig. S4. Although most mutations were on target, there were off-target mutations identified (Fig. 4C and fig. S5). For the *TRAC* sgRNA, there were low-abundance mutations within the transcriptional unit of *CLIC2* (chloride intracellular channel 2); however, disruption of *CLIC2* in T cells is not expected to have negative consequences because it is not reported to be expressed in T cells. For the *TRBC* sgRNA, off-target edits were identified in genes encoding a transcriptional regulator (ZNF609) and a long intergenic non–protein coding RNA (LINC00377) (table S3). In addition to the above post hoc investigations of multiplex editing specificity, all products were shown not to have cellular transformation by virtue of the absence of long-term growth before infusion (table S1).

Detection of chromosomal translocations in CRISPR-Cas9–engineered T cells

In addition to the above detection of repair of double-strand DNA breaks by NHEJ, on-target mutagenesis by engineered nucleases can result in deletions, duplications, inversions, and translocations and can also lead to complex chromosomal rearrangements under some conditions (*37*). CRISPR-Cas9 has been used to intentionally create oncogenic chromosomal rearrangements (*38*). In preclinical studies with human T cells, simultaneous gene editing of *TRAC* and *CD52* using TALENs led to translocations that were detected at frequencies of 10^{-4} to 10^{-2} (*39*). In a subsequent clinical report using dual-gene editing with TALENs, chromosomal rearrangements were observed in 4% of infused cells (*40*). To study the safety and genotoxicity of multiplex CRISPR-Cas9 genome editing on three chromosomes, we used stringent release criteria of the manufactured cells and assays to detect translocations (fig. S6). We developed and qualified quantitative PCR (qPCR) assays to quantify the 12 potential translocations that could occur with the simultaneous editing of four loci: *TRAC*, *TRBC1*, *TRBC2*, and *PDCD1* (see materials and methods). We observed translocations in all manufactured products; however, the translocations were at the limit of detection for the assay in patient UPN39 (Fig. 5A). *TRBC1:TRBC2* was the most abundant rearrangement (Fig. 5A), resulting in a 9.3-kb deletion (supplementary materials). The deletion and translocations peaked on days 5 to 7 of manufacturing and then declined in frequency until cell harvest. The translocations and the *TRBC1:TRBC2* deletion were evident in the three patients between 10 days after infusion and 30 to 170 days after infusion (Fig. 5B). However, the rearrangements declined in frequency in vivo, suggesting that they conferred no evidence of a growth advantage over many generations of expansion in the patients on this trial (Fig. 3, A and B). At days 30, 150, and 170 in patients UPN07, UPN35, and UPN39, respectively, chromosomal translocations were at the limits of detection or not detected for all rearrangements except for the 9.3-kb deletion for *TRBC1:TRBC2*.

Single-cell RNA sequencing analysis reveals evolution of CRISPR-Cas9–engineered NYCE cells

We used single-cell RNA sequencing (scRNA-seq) to comprehensively characterize the transcriptomic phenotype of the NYCE T cells and their evolution over time in patient UPN39 (fig. S7). UPN39 was chosen because they had the highest level of cell engraftment and because this patient had evidence of tumor regression. CRISPR-Cas9–engineered T cells were infused to patient UPN39 and recovered after infusion from the blood on day 10 and at ~4 months (day 113) and were analyzed by scRNA-seq, as described in the materials and methods. For each sample (infusion product, day 10 and day 113), T cells were sorted on the basis of expression of CD4 or CD8 and processed using droplet-based 5′ scRNA-seq. From the gene expression libraries, PCR was used to further amplify cellular cDNA corresponding to the NY-ESO-1 TCR transgene, as well as *TRAC*, *TRBC*, and *PDCD1* target sequences, allowing us to genotype single cells as wild type or mutant. In the infusion product, cells

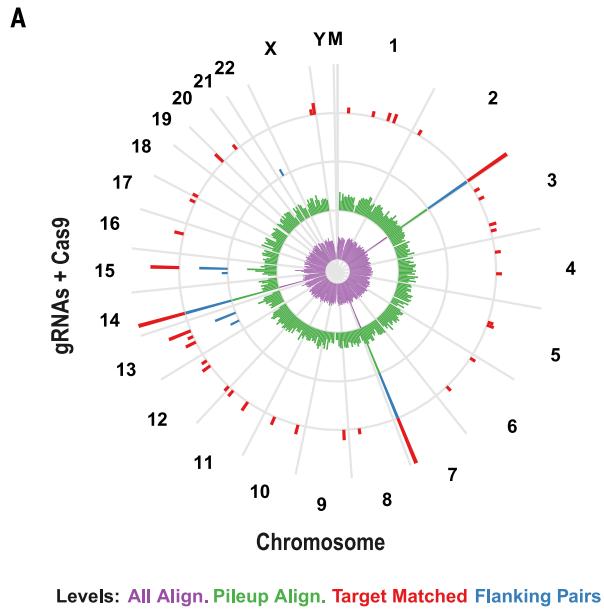

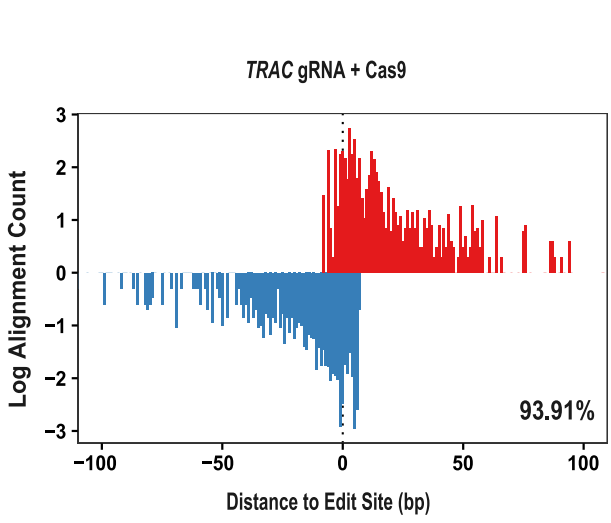

C

TRAC gRNA + Cas9

TGTGCTAGACATGAGGTCTANGG	Target	Abund.	Gene ID
. . . . . T. .	On	7,778	*TRA*~*
GA. . . A. . . . . A. . . . . A. .	Off	7	*CLIC2**
. TA. . . . . T. . TA. . . . TT. T	Off	6	*LINC00583*
C. G. . G. AT. . . . . A. GA.	Off	5	*C10orf67*
. T. AG. . . . . T. CA. C	Off	5	*LOC100131939*
. C. . . . TT. . T. A. A. . . . . CT.	Off	5	*ANKS1B**
. . . ATA. . G. . . . T. . . . G. G. T	Off	3	*IQCJ–SCHIP1**
. . . TT. . C. . . . A. C. . . . . G. .	Off	3	*ADCY10**
AA. . T. . . . . GA.	Off	2	*LDAH**
G. . . . . G. . . CAT. TCC.	Off	2	*MRPS27**

Fig. 4. Fidelity of CRISPR-Cas9 gene editing. (**A**) Genomic distribution of oligonucleotide (dsODN) incorporation sites, which mark locations of double-strand breaks. The ring indicates the human chromosomes aligned end to end, plus the mitochondrial chromosome (labeled M). The targeted cleavage sites are on chromosomes 2, 7, and 14. The frequency of cleavage and subsequent dsODN incorporation is shown on a log scale on each ring (pooled over 10-Mb windows). The purple innermost ring plots all alignments identified. The green ring shows pileups of three or more overlapping sequences, the blue ring shows alignments extending along either strand from a common dsODN incorporation site ("flanking pairs"), and the red ring shows reads with matches to the gRNA (allowing <6 mismatches) within 100 bp ("target matched"). (**B**) Distribution of inferred positions of cleavage and dsODN incorporation at an on-target locus. Incorporations in different strand orientations are shown on the positive (red) and negative (blue) *y* axis. The percentage in the bottom right corner is an estimate of the number of incorporations associated with the on-target site (based on pileups) captured within the allowed window of 100 bp. (**C**) Sequences of sites of cleavage and dsODN incorporation are shown, annotated by whether they are on target or off target ("Target"); the total number of unique alignments associated with the site ("Abund."); and an identifier indicating the nearest gene ("Gene ID"). An asterisk after the gene name indicates that the site is within the transcription unit of the specific gene, whereas "~" indicates that the gene appears on the allOnco cancer-associated gene list.

were identified that contained mutations in all three target sequences (Fig. 6, A and B). The most commonly mutated gene was *TRAC*. About 30% of cells had no mutations identified, whereas ~40% had one mutation, and ~20 and ~10% of the T cells in the manufactured product were double mutated and triple mutated, respectively, at the target sequences. Of the transgenic TCR$^+$ cells in the infusion product, monogenic mutations were less frequent than digenic and trigenic mutations (Fig. 6A). Single-cell genotyping of UPN39 cells at 10 days and 4 months after infusion showed a decline in the frequency of gene-edited T cells from the levels in the infusion product, and this decline occurred regardless of whether the cells were transduced with the NY-ESO-1 TCR (Fig. 6C). The frequency of gene-edited cells was quite stable between day 10 and 4 months postinfusion, and notably, about 40% of the peripheral blood–circulating T cells in this patient 4 months after infusion were mutated at any one of the targeted genes (Fig. 6, B and C, and table S4).

Of particular interest is the frequency and evolution of PD-1–deficient T cells owing to the previous mention that genetic disruption of *PDCD1* in CAR and TCR T cells enhances antitumor efficacy in preclinical models

(*19*, *21*–*24*). We found that ~25% of the T cells expressing the NY-ESO-1 TCR in the infusion product had mutations in the *PDCD1* locus (fig. S8). It is interesting that the frequency of cells with edits in the *PDCD1* locus decreased to ~5% of the cells expressing the transgenic TCR at 4 months postinfusion. This would be consistent with mouse studies of chronic infection in which PD-1–deficient T cells are less able to establish memory (*18*).

Figure 6D shows the distribution of engineered T cells expressing the NY-ESO-1 TCR transgene in the infusion product of patient UPN39, and again at 4 months in vivo as they evolve from the infused cells. In the heatmap (Fig. 6E), the most differentially expressed genes in the cells expressing the NY-ESO-1 transcript at the various time points are shown in table S5. Notably, UPN39 had increases in expression of genes associated with central memory (*IL7R* and *TCF7*) over time (Fig. 6, D and E, and table S4). This is in marked contrast to the recently published results with NY-ESO-1 T cells in the absence of genome editing, in which the infused transgenic T cells evolved to a terminally differentiated phenotype and displayed characteristics of T cell exhaustion in cancer patients (*12*).

Table 3. iGUIDE measurement of on-target editing efficiency for each gene by final product.

Manufactured NYCE T cell product (subject ID)	On-target editing efficiency (%)		
	PDCD1	*TRAC*	*TRBC*
UPN07	100.0	99.6	96.1
UPN27	99.6	99.1	96.8
UPN35	99.8	99.1	97.0
UPN39	98.2	96.7	93.5
Average ± SD	99.4 ± 0.8	98.6 ± 1.3	95.8 ± 1.6

Clinical observations

The clinical course of the three infused cancer patients is shown in Fig. 7 (and described in the materials and methods). No patient experienced cytokine release syndrome or overt side effects attributed to the cell infusion (table S5). The best clinical responses were stable disease in two patients. UPN39 had a mixed response, with a ~50% decrease in a large abdominal mass that was sustained for 4 months (Fig. 7D), although other lesions progressed. As of December 2019, all patients have progressed: Two are receiving other therapies, and UPN07 died from progressive myeloma.

Biopsies of bone marrow and tumor showed trafficking of the NYCE-engineered T cells to the sites of tumor in all three patients (Fig. 3A). It is interesting to note that even though the tumor biopsies revealed residual tumor, in both patients with myeloma, there was a reduction

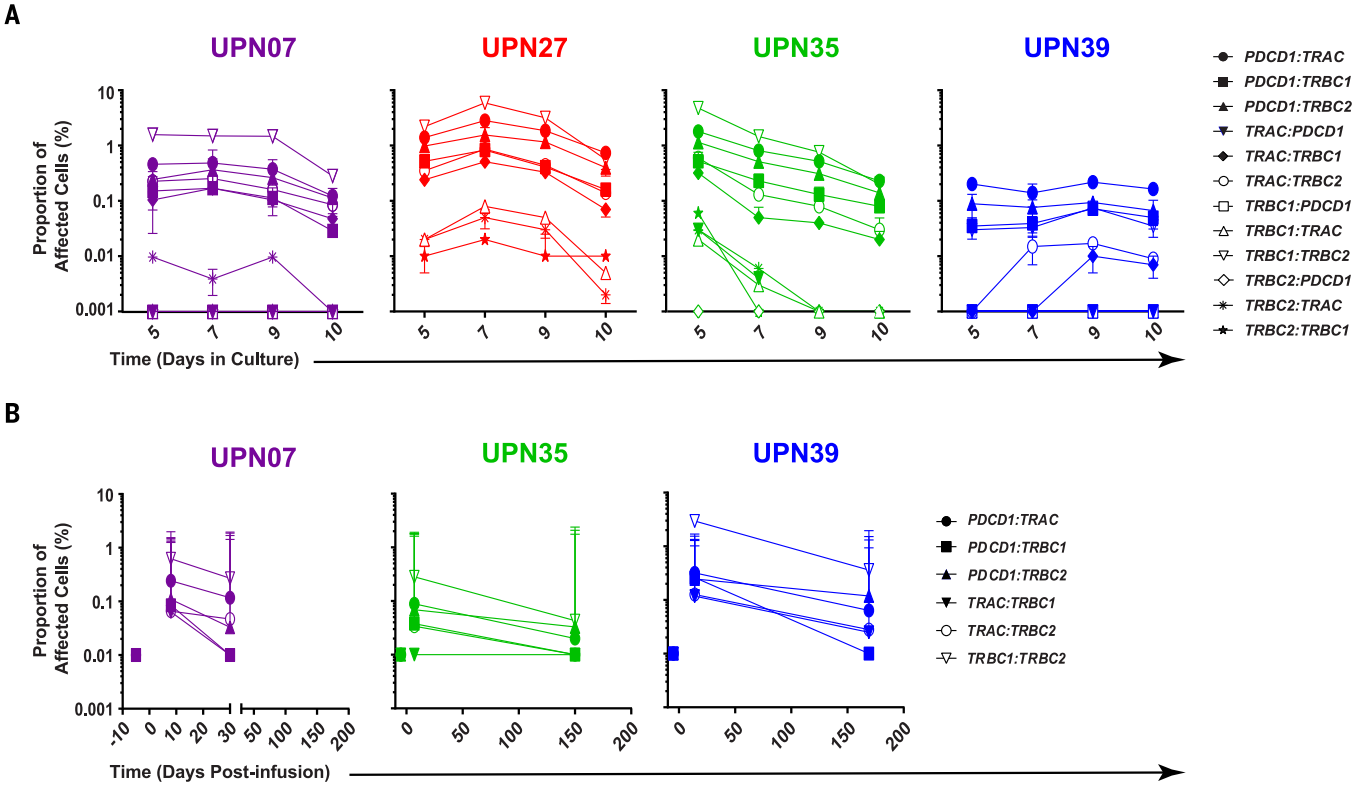

Fig. 5. Detection of chromosomal translocations in engineered T cells after CRISPR-Cas9 gene editing. (**A**) Evaluation of chromosomal translocations in NYCE T cell infusion products during the course of large-scale culture is shown. For the 12 monocentromeric translocation assays conducted, a positive reference sample that contains 1×10^3 copies of the synthetic template plasmid was evaluated as a control, and the percent difference between expected and observed marking was calculated. The absence of amplification from the 12 reactions that correspond to the different chromosomal translocations indicates assay specificity (see methods). (**B**) Longitudinal analysis of chromosomal translocations in vivo in three patients pre– and post–NYCE T cell product infusion is displayed. In (A) and (B), error bars represent SD. For graphical purposes, the proportions of affected cells were plotted on a log scale; a value of 0.001% indicates that translocations were not detected.

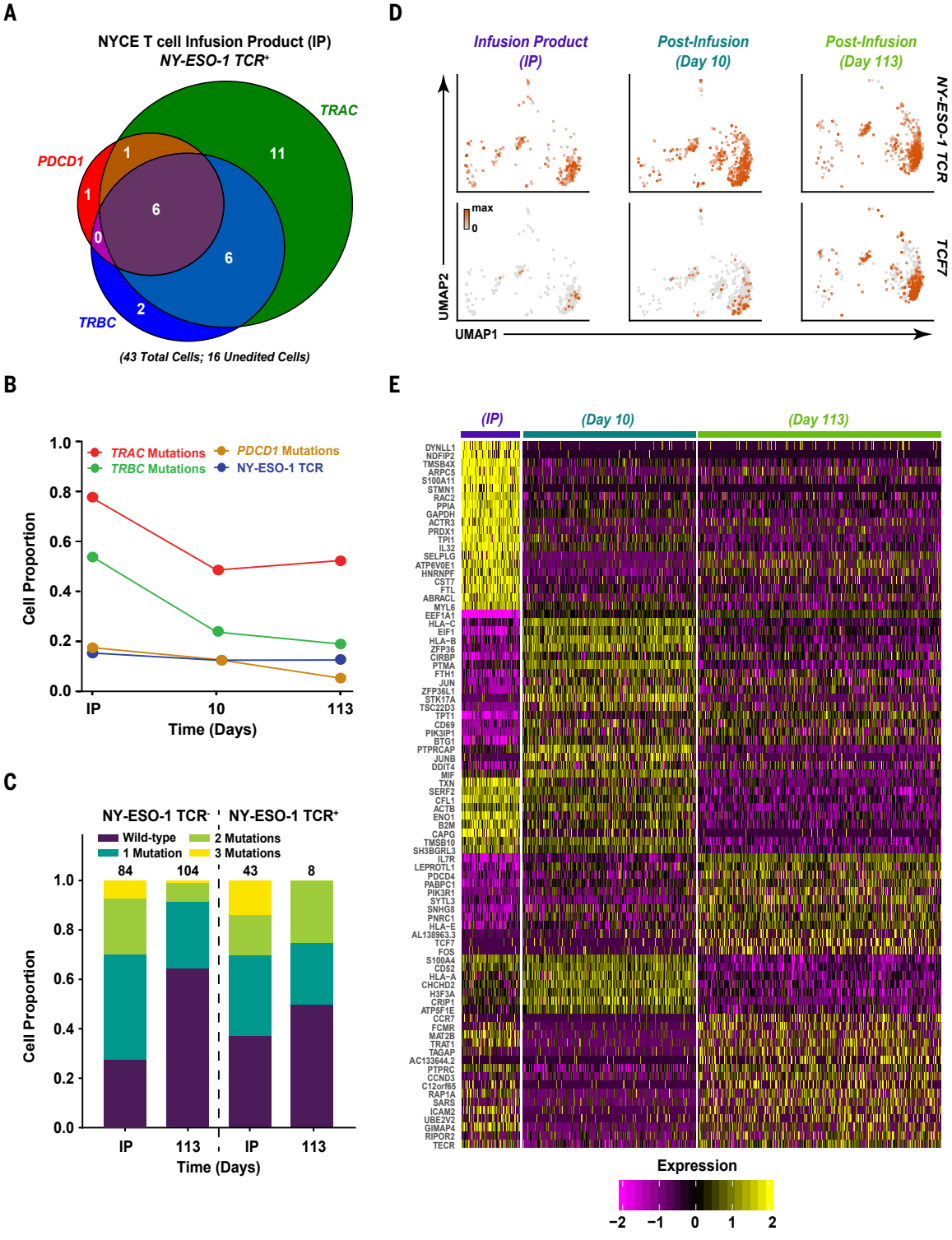

Fig. 6. Single-cell RNA sequencing of patient UPN39 CRISPR-Cas9–engineered NYCE T cells pre- and postinfusion. (**A**) Venn diagram showing relative numbers of NY-ESO-1 TCR–positive cells with *TRAC*, *TRBC*, and/or *PDCD1* mutations in the NYCE T cell infusion product (IP) (day 0). (**B**) Proportions of preinfusion (IP, day 0) and postinfusion (days 10 and 113) wild-type T cells with *TRAC*, *TRBC*, or *PDCD1* mutations or expressing the NY-ESO-1 TCR transgene. Numbers of cells belonging to each of these categories are listed below the graph. (**C**) Analysis of NY-ESO-1 TCR–positive (right) and NY-ESO-1 TCR–negative (left) cells without mutations (wild type) or with single, double, or triple mutations at day 0 (NYCE T cell infusion product) and day 113 post–NYCE T cell infusion. Numbers of analyzed cells for each time point are listed above the bars. (**D**) Uniform manifold approximation and projection (UMAP) plots of gene expression data. Analysis was performed on all T cells integrated across time points, but only NY-ESO-1 TCR–expressing cells, split by time point, are shown (top). The increase in *TCF7* expression is indicative of an acquired central memory phenotype (bottom, same cells). (**E**) Heatmap showing scaled expression of differentially expressed genes in NY-ESO-1 TCR–positive T cells across time points. Color scheme is based on scaled gene expression from −2 (purple) to 2 (yellow).

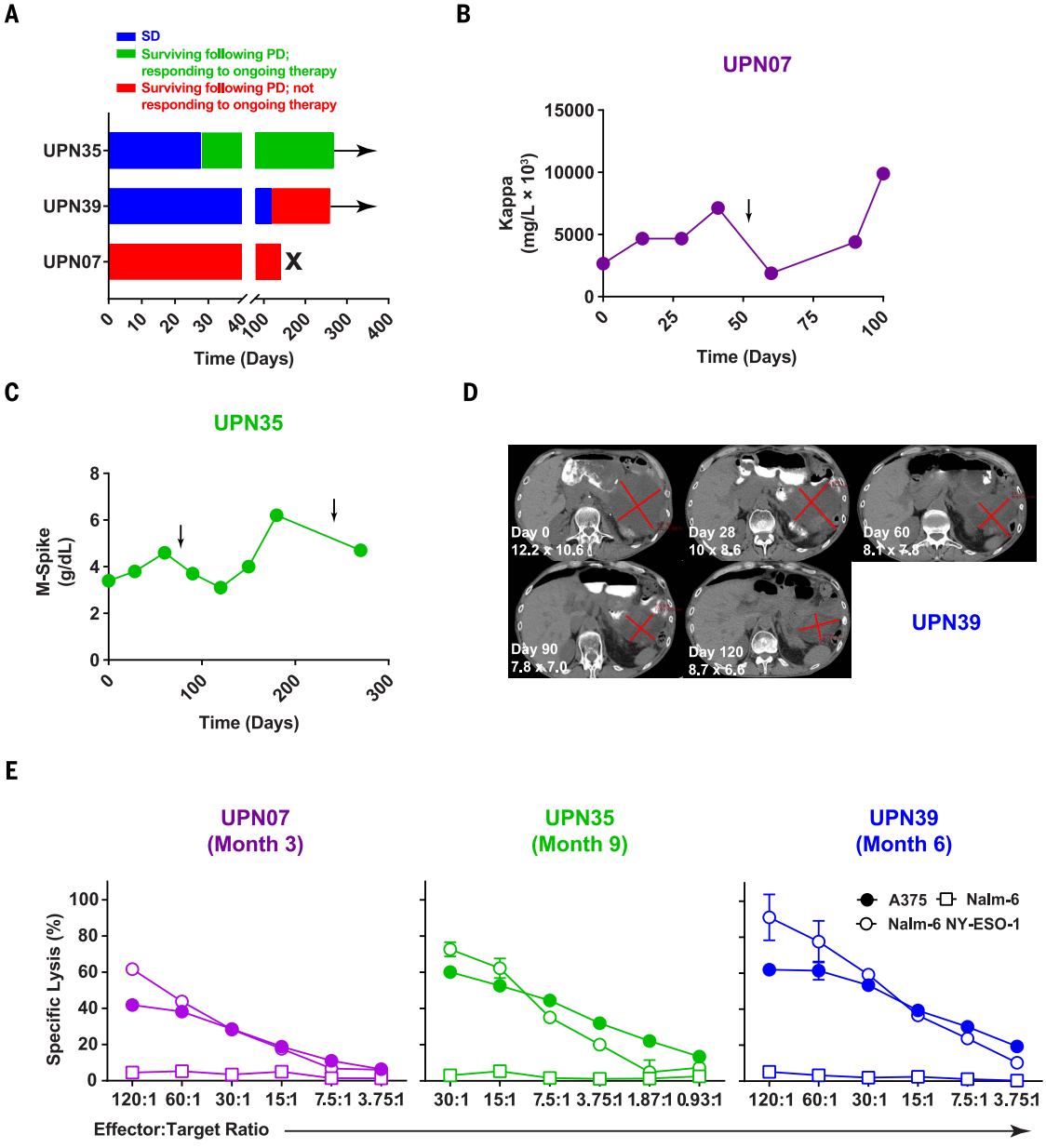

Fig. 7. Clinical responses and patient outcomes after infusion of CRISPR-Cas9–engineered NYCE T cells. (**A**) Swimmer's plot describing time on study for each patient, duration of follow-up off study (defined as survival beyond progression or initiation of other cancer therapy), and present status (differentially colored) is shown. Arrows indicate ongoing survival. SD, stable disease; PD, progressive disease. (**B**) Changes in kappa light chain levels (mg/liter × 10^3) in patient UPN07 after NYCE T cell product infusion are depicted. Vertical black arrow indicates initiation of a D-ACE salvage chemotherapy regimen (defined as intravenous infusion of cisplatin, etoposide, cytarabine, and dexamethasone). (**C**) Longitudinal M-spike levels (g/dl) in patient UPN35 post–NYCE T cell product administration are shown. Vertical black arrows indicate administration of combination therapy with elotuzumab, pomalidomide, and dexamethasone. (**D**) Computed tomography scans demonstrating tumor regression in patient UPN39 after administration of an autologous NYCE T cell infusion product. Radiologic studies were obtained before therapy and after adoptive transfer of NYCE T cells. Tumor is indicated by red X. (**E**) Cytolytic capacity of NY-ESO-1–specific $CD8^+$ T cells recovered at the indicated month after infusion and expanded from patients is shown. PBMC samples collected after NYCE T cell product infusion were expanded in vitro in the presence of NY-ESO-1 peptide and interleukin-2. The ability of expanded effector cells to recognize antigen and elicit cytotoxicity was tested in a 4-hour ^{51}Cr release assay incorporating Nalm-6 NY-ESO-1^+, parental Nalm-6 (NY-ESO-1^-), and A375 melanoma cells (NY-ESO-1^+). All target cell lines were HLA-A*02 positive. Assays were performed in triplicate, and error bars represent SD.

in the target antigens NY-ESO-1 and/or LAGE-1 (fig. S9). The reduction of target antigen was transient in patient UPN07 and persistent in patient UPN35. This result is consistent with an on-target effect of the infused cells, likely resulting in tumor editing (*41*).

To determine whether the NYCE cells retained antitumor activity after infusion, samples of blood obtained from patients 3 to 9 months after infusion were expanded in culture in the presence of NY-ESO-1 peptide and assessed for cytotoxicity against tumor cells (Fig. 7E and fig. S10). Antigen-specific cytotoxicity was observed in all three patients. It is interesting to note that the most potent antitumor cytotoxicity was observed in UPN39, because UPN39 was the only patient to have tumor regression after infusion of the CRISPR-Cas9–engineered T cells (Fig. 7D).

Discussion

Our phase 1 first-in-human pilot study demonstrates the initial safety and feasibility of multiplex CRISPR-Cas9 T cell human genome engineering in patients with advanced, refractory cancer. In one patient analyzed at depth, a frequency of 30% of digenic and trigenic editing was achieved in the infused cell population, and 20% of the TCR transgenic T cells in circulation 4 months later had persisting digenic and trigenic edits. We chose to redirect specificity of the T cells with a T cell receptor, rather than a CAR, to avoid the CAR-associated potential toxicities such as cytokine release syndrome (*31*). This provided a lower baseline toxicity profile, thus enhancing the ability to detect toxicity specifically associated with the CRISPR-Cas9–engineering process. We observed mild toxicity, and most of the adverse events were attributed to the lymphodepleting chemotherapy. We note that although the initial clinical results have acceptable safety, experience with more patients given infusions of CRISPR-engineered T cells with higher editing efficiencies, and longer observation after infusion, will be required to fully assess the safety of this approach.

Our large-scale product manufacturing process resulted in gene-editing efficiencies similar to those in our preclinical studies (*24*). A surprising finding was the high-level engraftment and long-term persistence of the infused CRISPR-Cas9–engineered T cells. In previous clinical studies testing adoptively transferred NY-ESO-1 transgenic T cells, the engrafted cells had an initial decay half-life of about 1 week (*10*–*12*). The explanation for the extended survival that we observed remains to be determined and could include the editing of the endogenous TCR, PD-1, and/or the choice of the TCR and vector design.

The use of scRNA-seq technology permitted the analysis of the transcriptome of the infused NY-ESO-1–specific T cells (i.e., CRISPR-Cas9–engineered T cells) at baseline and for up to 4 months in vivo. The results shown for UPN39 revealed that the infused cells evolved to a state consistent with central memory. These results are in contrast to a recent study in which the infused NY-ESO-1 T cells evolved to a state consistent with T cell exhaustion (*12*). A limitation of our in vivo single-cell analysis is that for purposes of feasibility, it is limited to the one patient who had the highest level of engraftment. Another limitation is that we were not able to compare the transcriptional state of the modified cells in the tumor microenvironment with circulating NYCE T cells.

Analysis of the manufacturing process in vitro demonstrated monochromosomal translocations and rearrangements, and some of these persisted in vivo. The translocations were not random in occurrence and occurred most frequently between *PDCD1:TRAC* and *TRBC1:TRBC2*. The frequency of translocations that we observed with trigenic editing is similar to that reported for digenic editing using TALEN-mediated gene editing in preclinical and clinical studies, in which rearrangements were detected in about 4% of cells (*39*, *40*). It is important to note that healthy individuals often harbor oncogenic translocations in B and T cells (*42*–*44*). T cells bearing translocations can persist for months to years without evidence of pathogenicity (*45*–*47*).

Antagonism of the PD-1:PD-L1 costimulatory pathway can result in organ-specific and systemic autoimmunity (*17*, *48*). PD-1 has been reported to function as a haploinsufficient tumor suppressor in mouse T cells (*49*). Our patients have had engraftment with PD-1–deficient T cells, and to date, there is no evidence of autoimmunity or T cell genotoxicity.

In conclusion, our phase 1 human pilot study has confirmed that multiplex CRISPR-Cas9 editing of the human genome is possible at clinical scale. We note that although the initial clinical results suggest that this treatment is safe, experience with more patients given infusions with higher editing efficiencies and longer observation after infusion will be required to fully assess the safety of this approach. The potential rejection of infused cells due to preexisting immune responses to Cas9 (*28*, *29*) does not appear to be a barrier to the application of this promising technology. Finally, it is important to note that our manufacturing was based on the reagents available in 2016, when our protocol had been reviewed by the National Institutes of Health (NIH) Recombinant DNA Advisory Committee and received approval. Our Investigational New Drug application was subsequently reviewed and accepted by the FDA. There has been rapid progress in the field since that time, with the development of reagents that should increase efficiencies and decrease off-target editing using CRISPR-based technology (*50*).

Materials and methods summary

Experimental design

The clinical protocol is listed at clinicaltrials.gov, trial NCT03399448. Protocol no. 1604-1524 "Phase 1 trial of autologous T cells engineered to express NY-ESO-1 TCR and CRISPR gene edited to eliminate endogenous TCR and PD-1 (NYCE T Cells)" was reviewed and approved by the U.S. National Institutes of Health Recombinant DNA Advisory Committee on 21 June 2016. See fig. S1B for clinical trial design. Patient demographics are shown in Table 1. A list of adverse events is depicted in Table 2.

Guide RNAs (gRNAs)

The genomic gRNA target sequences with protospacer adjacent motif (PAM) underlined were: *TRAC1* and *TRAC2*: 5′-TGTGCTAGACATGAGGTCTATGG-3′, *TRBC*: 5′-GGAGAATGACGAGTGGACCCAGG-3′, and *PDCD1*: 5′-GGCGCCCTGGCCAGTCGTCTGGG-3′. In vitro transcribed gRNA was prepared from linearized DNA (Aldevron) using Bulk T7 Megascript 5X (Ambion) and purified using RNeasy Maxi Kit (Qiagen).

Recombinant Cas9 protein

Cas9 recombinant protein derived from *S. pyogenes* was TrueCut Cas9 v2 (catalogue no. A36499, ThermoFisher). Cas9 RNP was made by incubating protein with gRNA at a molar ratio of 1:1 at 25°C for 10 min immediately before electroporation.

Lentiviral vector manufacturing

The 8F TCR recognizes the HLA-A*0201 SLLMWITQC epitope on NY-ESO-1 and LAGE-1. The 8F TCR was isolated from a T cell clone obtained from patient after vaccination with NY-ESO-1 peptide. The TCR sequences were cloned into a transfer plasmid that contains the EF-1α promoter, a cPPT sequence, a Rev response element and a woodchuck hepatitis virus posttranscriptional regulatory element (WPRE), as shown in fig. S1B. Plasmid DNA was manufactured at Puresyn, Inc. Lentiviral vector was produced at the University of Pennsylvania Center for Advanced Retinal and Ocular Therapeutics using transient transfection with four plasmids expressing the transfer vector, Rev, VSV-G, and gag-pol, in human embryonic kidney 293T cells.

REFERENCES AND NOTES

1. P. Rouet, F. Smih, M. Jasin, Introduction of double-strand breaks into the genome of mouse cells by expression of a rare-cutting endonuclease. *Mol. Cell. Biol.* **14**, 8096–8106 (1994). doi: 10.1128/MCB.14.12.8096; pmid: 7969147
2. M. H. Porteus, A new class of medicines through DNA editing. *N. Engl. J. Med.* **380**, 947–959 (2019). doi: 10.1056/NEJMra1800729; pmid: 30855744
3. P. Tebas *et al.*, Gene editing of *CCR5* in autologous CD4 T cells of persons infected with HIV. *N. Engl. J. Med.* **370**, 901–910 (2014). doi: 10.1056/NEJMoa1300662; pmid: 24597865
4. L. Xu *et al.*, CRISPR-edited stem cells in a patient with HIV and acute lymphocytic leukemia. *N. Engl. J. Med.* **381**, 1240–1247 (2019). doi: 10.1056/NEJMoa1817426; pmid: 31509667
5. M. Jinek *et al.*, A programmable dual-RNA-guided DNA endonuclease in adaptive bacterial immunity. *Science* **337**, 816–821 (2012). doi: 10.1126/science.1225829; pmid: 22745249
6. L. Cong *et al.*, Multiplex genome engineering using CRISPR/Cas systems. *Science* **339**, 819–823 (2013). doi: 10.1126/science.1231143; pmid: 23287718
7. P. K. Mandal *et al.*, Efficient ablation of genes in human hematopoietic stem and effector cells using CRISPR/Cas9. *Cell Stem Cell* **15**, 643–652 (2014). doi: 10.1016/j.stem.2014.10.004; pmid: 25517468
8. J. F. Hultquist *et al.*, CRISPR-Cas9 genome engineering of primary CD4$^+$ T cells for the interrogation of HIV-host factor interactions. *Nat. Protoc.* **14**, 1–27 (2019). doi: 10.1038/s41596-018-0069-7; pmid: 30559373
9. R. O. Bak *et al.*, Multiplexed genetic engineering of human hematopoietic stem and progenitor cells using CRISPR/Cas9 and AAV6. *eLife* **6**, e27873 (2017). doi: 10.7554/eLife.27873; pmid: 28956530
10. P. F. Robbins *et al.*, Tumor regression in patients with metastatic synovial cell sarcoma and melanoma using genetically engineered lymphocytes reactive with NY-ESO-1. *J. Clin. Oncol.* **29**, 917–924 (2011). doi: 10.1200/JCO.2010.32.2537; pmid: 21282551

11. A. P. Rapoport *et al*., NY-ESO-1-specific TCR-engineered T cells mediate sustained antigen-specific antitumor effects in myeloma. *Nat. Med.* **21**, 914–921 (2015). doi: 10.1038/nm.3910; pmid: 26193344
12. T. S. Nowicki *et al*., A pilot trial of the combination of transgenic NY-ESO-1-reactive adoptive cellular therapy with dendritic cell vaccination with or without ipilimumab. *Clin. Cancer Res.* **25**, 2096–2108 (2019). doi: 10.1158/1078-0432.CCR-18-3496; pmid: 30573690
13. E. Provasi *et al*., Editing T cell specificity towards leukemia by zinc finger nucleases and lentiviral gene transfer. *Nat. Med.* **18**, 807–815 (2012). doi: 10.1038/nm.2128; pmid: 20400962
14. G. M. Bendle *et al*., Lethal graft-versus-host disease in mouse models of T cell receptor gene therapy. *Nat. Med.* **16**, 565–570, 1p, 570 (2010). doi: 10.1038/nm.2128; pmid: 20400962
15. K. Schober *et al*., Orthotopic replacement of T-cell receptor α- and β-chains with preservation of near-physiological T-cell function. *Nat. Biomed. Eng.* **3**, 974–984 (2019). doi: 10.1038/s41551-019-0409-0; pmid: 31182835
16. A. Schietinger, J. J. Delrow, R. S. Basom, J. N. Blattman, P. D. Greenberg, Rescued tolerant CD8 T cells are preprogrammed to reestablish the tolerant state. *Science* **335**, 723–727 (2012). doi: 10.1126/science.1214277; pmid: 22267581
17. H. Nishimura, M. Nose, H. Hiai, N. Minato, T. Honjo, Development of lupus-like autoimmune diseases by disruption of the PD-1 gene encoding an ITIM motif-carrying immunoreceptor. *Immunity* **11**, 141–151 (1999). doi: 10.1016/S1074-7613(00)80089-8; pmid: 10485649
18. P. M. Odorizzi, K. E. Pauken, M. A. Paley, A. Sharpe, E. J. Wherry, Genetic absence of PD-1 promotes accumulation of terminally differentiated exhausted $CD8^+$ T cells. *J. Exp. Med.* **212**, 1125–1137 (2015). doi: 10.1084/jem.20142237; pmid: 26034050
19. L. J. Rupp *et al*., CRISPR/Cas9-mediated PD-1 disruption enhances anti-tumor efficacy of human chimeric antigen receptor T cells. *Sci. Rep.* **7**, 737 (2017). doi: 10.1038/s41598-017-00462-8; pmid: 28389661
20. I. Serganova *et al*., Enhancement of PSMA-directed CAR adoptive immunotherapy by PD-1/PD-L1 blockade. *Mol. Ther. Oncolytics* **4**, 41–54 (2016). doi: 10.1016/j.omto.2016.11.005; pmid: 28345023
21. S. Su *et al*., CRISPR-Cas9 mediated efficient PD-1 disruption on human primary T cells from cancer patients. *Sci. Rep.* **6**, 20070 (2016). doi: 10.1038/srep20070; pmid: 26818188
22. L. Menger *et al*., TALEN-mediated inactivation of PD-1 in tumor-reactive lymphocytes promotes intratumoral T-cell persistence and rejection of established tumors. *Cancer Res.* **76**, 2087–2093 (2016). doi: 10.1158/0008-5472.CAN-15-3352; pmid: 27197251
23. L. Cherkassky *et al*., Human CAR T cells with cell-intrinsic PD-1 checkpoint blockade resist tumor-mediated inhibition. *J. Clin. Invest.* **126**, 3130–3144 (2016). doi: 10.1172/JCI83092; pmid: 27454297
24. J. Ren *et al*., Multiplex genome editing to generate universal CAR T cells resistant to PD1 inhibition. *Clin. Cancer Res.* **23**, 2255–2266 (2017). doi: 10.1158/1078-0432.CCR-16-1300; pmid: 27815355
25. J. Ren *et al*., A versatile system for rapid multiplex genome-edited CAR T cell generation. *Oncotarget* **8**, 17002–17011 (2017). doi: 10.18632/oncotarget.15218; pmid: 28199983
26. X. Liu *et al*., CRISPR-Cas9-mediated multiplex gene editing in CAR-T cells. *Cell Res.* **27**, 154–157 (2017). doi: 10.1038/cr.2016.142; pmid: 27910851
27. E. K. Moon *et al*., Blockade of programmed death 1 augments the ability of human T cells engineered to target NY-ESO-1 to control tumor growth after adoptive transfer. *Clin. Cancer Res.* **22**, 436–447 (2016). doi: 10.1158/1078-0432.CCR-15-1070; pmid: 26324743
28. C. T. Charlesworth *et al*., Identification of preexisting adaptive immunity to Cas9 proteins in humans. *Nat. Med.* **25**, 249–254 (2019). doi: 10.1038/s41591-018-0326-x; pmid: 30692695
29. D. L. Wagner *et al*., High prevalence of *Streptococcus pyogenes* Cas9-reactive T cells within the adult human population. *Nat. Med.* **25**, 242–248 (2019). doi: 10.1038/s41591-018-0204-6; pmid: 30374197
30. V. L. Simhadri *et al*., Prevalence of pre-existing antibodies to CRISPR-associated nuclease Cas9 in the USA population. *Mol. Ther. Methods Clin. Dev.* **10**, 105–112 (2018). doi: 10.1016/j.omtm.2018.06.006; pmid: 30073181
31. D. T. Teachey *et al*., Identification of predictive biomarkers for cytokine release syndrome after chimeric antigen receptor T-cell therapy for acute lymphoblastic leukemia. *Cancer Discov.* **6**, 664–679 (2016). doi: 10.1158/2159-8290.CD-16-0040; pmid: 27076371
32. P. F. Robbins *et al*., A pilot trial using lymphocytes genetically engineered with an NY-ESO-1-reactive T-cell receptor: Long-term follow-up and correlates with response. *Clin. Cancer Res.* **21**, 1019–1027 (2015). doi: 10.1158/1078-0432.CCR-14-2708; pmid: 25538264
33. S. P. D'Angelo *et al*., Antitumor activity associated with prolonged persistence of adoptively transferred NY-ESO-1 ^{c259}T cells in synovial sarcoma. *Cancer Discov.* **8**, 944–957 (2018). doi: 10.1158/2159-8290.CD-17-1417; pmid: 29891538
34. C. L. Nobles *et al*., iGUIDE: An improved pipeline for analyzing CRISPR cleavage specificity. *Genome Biol.* **20**, 14 (2019). doi: 10.1186/s13059-019-1625-3; pmid: 30654827
35. S. Q. Tsai *et al*., GUIDE-seq enables genome-wide profiling of off-target cleavage by CRISPR-Cas nucleases. *Nat. Biotechnol.* **33**, 187–197 (2015). doi: 10.1038/nbt.3117; pmid: 25513782
36. M. M. Vilenchik, A. G. Knudson, Endogenous DNA double-strand breaks: Production, fidelity of repair, and induction of cancer. *Proc. Natl. Acad. Sci. U.S.A.* **100**, 12871–12876 (2003). doi: 10.1073/pnas.2135498100; pmid: 14566050
37. M. Kosicki, K. Tomberg, A. Bradley, Repair of double-strand breaks induced by CRISPR-Cas9 leads to large deletions and complex rearrangements. *Nat. Biotechnol.* **36**, 765–771 (2018). doi: 10.1038/nbt.4192; pmid: 30010673
38. D. Maddalo *et al*., In vivo engineering of oncogenic chromosomal rearrangements with the CRISPR/Cas9 system. *Nature* **516**, 423–427 (2014). doi: 10.1038/nature13902; pmid: 25337876
39. L. Poirot *et al*., Multiplex genome-edited T-cell manufacturing platform for "off-the-shelf" adoptive T-cell immunotherapies. *Cancer Res.* **75**, 3853–3864 (2015). doi: 10.1158/0008-5472.CAN-14-3321; pmid: 26183927
40. W. Qasim *et al*., Molecular remission of infant B-ALL after infusion of universal TALEN gene-edited CAR T cells. *Sci. Transl. Med.* **9**, eaaj2013 (2017). doi: 10.1126/scitranslmed.aaj2013; pmid: 28123068
41. G. P. Dunn, A. T. Bruce, H. Ikeda, L. J. Old, R. D. Schreiber, Cancer immunoediting: From immunosurveillance to tumor escape. *Nat. Immunol.* **3**, 991–998 (2002). doi: 10.1038/ni1102-991; pmid: 12407406
42. J. Bäsecke, F. Griesinger, L. Trümper, G. Brittinger, Leukemia- and lymphoma-associated genetic aberrations in healthy individuals. *Ann. Hematol.* **81**, 64–75 (2002). doi: 10.1007/s00277-002-0427-x; pmid: 11907785
43. S. I. Ismail, R. G. Naffa, A. M. Yousef, M. T. Ghanim, Incidence of bcr-abl fusion transcripts in healthy individuals. *Mol. Med. Rep.* **9**, 1271–1276 (2014). doi: 10.3892/mmr.2014.1951; pmid: 24535287
44. R. Chiarle, Translocations in normal B cells and cancers: Insights from new technical approaches. *Adv. Immunol.* **117**, 39–71 (2013). doi: 10.1016/B978-0-12-410524-9.00002-5; pmid: 23611285
45. C. A. Michie, A. McLean, C. Alcock, P. C. Beverley, Lifespan of human lymphocyte subsets defined by CD45 isoforms. *Nature* **360**, 264–265 (1992). doi: 10.1038/360264a0; pmid: 1436108
46. A. R. Mclean, C. A. Michie, In vivo estimates of division and death rates of human T lymphocytes. *Proc. Natl. Acad. Sci. U.S.A.* **92**, 3707–3711 (1995). doi: 10.1073/pnas.92.9.3707; pmid: 7731969
47. K. George, L. J. Chappell, F. A. Cucinotta, Persistence of space radiation induced cytogenetic damage in the blood lymphocytes of astronauts. *Mutat. Res.* **701**, 75–79 (2010). doi: 10.1016/j.mrgentox.2010.02.007; pmid: 20176126
48. C. H. June, J. T. Warshauer, J. A. Bluestone, Is autoimmunity the Achilles' heel of cancer immunotherapy? *Nat. Med.* **23**, 540–547 (2017). doi: 10.1038/nm.4321; pmid: 28475571
49. T. Wartewig *et al*., PD-1 is a haploinsufficient suppressor of T cell lymphomagenesis. *Nature* **552**, 121–125 (2017). doi: 10.1038/nature24649; pmid: 29143824
50. C. A. Vakulskas *et al*., A high-fidelity Cas9 mutant delivered as a ribonucleoprotein complex enables efficient gene editing in human hematopoietic stem and progenitor cells. *Nat. Med.* **24**, 1216–1224 (2018). doi: 10.1038/s41591-018-0137-0; pmid: 30082871

ACKNOWLEDGMENTS

We thank the Human Immunology Core at the University of Pennsylvania for providing leukocytes for research; the Clinical Cell and Vaccine Production Facility for GMP cell manufacturing; the Hospital of the University of Pennsylvania Apheresis Unit for peripheral blood mononuclear cell collections from which NYCE T cells were manufactured; regulatory assistance from E. Meagher, S. Emmanuel, E. Veloso, and the Office of Clinical Research, the Center for Advanced Retinal and Ocular Therapeutics Clinical Vector Core (CAROT CVC); RECIST Core for radiologic assessment of response; Data Safety Monitoring Board consisting of L. Schuchter, A. Rapoport, and M. Dhodapkar; J. Everett for data analysis with iGUIDE; C. Bartoszek, J. Finklestein, M. Gohil, A. Kim, N. Koterba, M. Mahir, B. Menchel, T. Mikheeva, F. Nazimuddin, H. Parakandi, R. Reynolds, M. Feldman, and T. Yoder for experimental support; W. Gladney for protocol development and management; and R. Chiarle at the Boston Children's Hospital for helpful discussions. **Funding:** This work was funded by the National Institutes of Health (grant 2R01CA120409 to Y.Z. and C.H.J.), Alliance for Cancer Gene Therapy Investigator's Award (J.A.F. and R.M.Y.), NCI P01 CA214278 (J.A.F., R.M.Y., S.F.L., and C.H.J.), NCI U54 CA24711 (J.A.F., M.M.D., R.M.Y., and C.H.J.), NIA U01 AG066100 (J.A.F., R.M.Y., and C.H.J.), NSF Engineering Research Center for Cell Manufacturing Technologies Seed Grant (J.A.F. and B.L.L.), Abramson Cancer Center Emerging Cancer Informatics Center of Excellence Award (J.A.F.), and sponsored research grants from the Parker Institute for Cancer Immunotherapy and Tmunity Therapeutics. **Author contributions:** Conceptualization: Y.Z., C.H.J., F.D.B.; Data curation: V.E.G.; Formal analysis: W.-T.H., J.A.F.; Funding acquisition: C.H.J.; Investigation: E.A.S., A.Ce., K.L.W., A.D.C., E.L., P.A.M., I.K., M.G., J.X., I.J., J.S., T.M., A.Ch., A.L.G., S.D., A.L., K.R.P., Y.Q., A.T.S., H.Y.C., B.M.C.; Methodology: L.T., A.F., J.S.-M., F.D.B.; Project administration: R.M.Y., A.C., G.P., J.K.J.; Software: C.L.N.; Supervision: J.A.F., S.F.L., E.O.H., J.J.M., R.M.Y., D.L.S.; Validation: V.E.G., F.C., L.T., M.M.D., S.F.L., J.S.-M.; Writing – original draft: E.A.S., J.A.F., S.F.L., C.H.J.; Writing – review and editing: B.L.L., D.L.S., H.Y.C., F.D.B. **Competing interests:** Y.Z. and C.H.J. are inventors on patent applications 15/516,052 and WO2016069282A1 submitted by the University of Pennsylvania that cover the use of gene modification in T cells for adoptive cell therapy. A.C., B.L.L., Y.Z., and C.H.J. are scientific founders of Tmunity and have equity in Tmunity. J.A.F. and M.M.D. have funding support from Tmunity. A.T.S. is a scientific founder of Immunai and has funding support from Arsenal Biosciences. S.F.L. has funding support from Tmunity, Cabaletta, and Novartis and is a consultant for Gilead/Kite. H.Y.C. is a co-founder of Accent Therapeutics and Boundless Bio and is a consultant for 10x Genomics, Arsenal Biosciences, and Spring Discovery. The other authors declare no competing interests. **Data and materials availability:** iGUIDE-seq data have been deposited with links to BioProject accession number PRJNA601142 in the NCBI BioProject database (https://www.ncbi.nlm.nih.gov/bioproject/). scRNA-seq data have been deposited into the database of Genotypes and Phenotypes dbGaP (https://www.ncbi.nlm.nih.gov/gap/) under accession number phs001707. Reagents are available under an MTA with the University of Pennsylvania; address requests to C.H.J.

SUPPLEMENTARY MATERIALS

science.sciencemag.org/content/367/6481/eaba7365/suppl/DC1
Materials and Methods
Supplementary Text
Figs. S1 to S10
Tables S1 to S6
References (*51*–*55*)

View/request a protocol for this paper from *Bio-protocol*.

3 January 2020; accepted 28 January 2020
Published online 6 February 2020
10.1126/science.aba7365

Science

CRISPR-engineered T cells in patients with refractory cancer

Edward A. Stadtmauer, Joseph A. Fraietta, Megan M. Davis, Adam D. Cohen, Kristy L. Weber, Eric Lancaster, Patricia A. Mangan, Irina Kulikovskaya, Minnal Gupta, Fang Chen, Lifeng Tian, Vanessa E. Gonzalez, Jun Xu, In-young Jung, J. Joseph Melenhorst, Gabriela Plesa, Joanne Shea, Tina Matlawski, Amanda Cervini, Avery L. Gaymon, Stephanie Desjardins, Anne Lamontagne, January Salas-Mckee, Andrew Fesnak, Donald L. Siegel, Bruce L. Levine, Julie K. Jadlowsky, Regina M. Young, Anne Chew, Wei-Ting Hwang, Elizabeth O. Hexner, Beatriz M. Carreno, Christopher L. Nobles, Frederic D. Bushman, Kevin R. Parker, Yanyan Qi, Ansuman T. Satpathy, Howard Y. Chang, Yangbing Zhao, Simon F. Lacey and Carl H. June

Science **367** (6481), eaba7365.
DOI: 10.1126/science.aba7365originally published online February 6, 2020

CRISPR takes first steps in humans

CRISPR-Cas9 is a revolutionary gene-editing technology that offers the potential to treat diseases such as cancer, but the effects of CRISPR in patients are currently unknown. Stadtmauer *et al.* report a phase 1 clinical trial to assess the safety and feasibility of CRISPR-Cas9 gene editing in three patients with advanced cancer (see the Perspective by Hamilton and Doudna). They removed immune cells called T lymphocytes from patients and used CRISPR-Cas9 to disrupt three genes (*TRAC, TRBC*, and *PDCD1*) with the goal of improving antitumor immunity. A cancer-targeting transgene, NY-ESO-1, was also introduced to recognize tumors. The engineered cells were administered to patients and were well tolerated, with durable engraftment observed for the study duration. These encouraging observations pave the way for future trials to study CRISPR-engineered cancer immunotherapies.

Science, this issue p. eaba7365; see also p. 976

Science (print ISSN 0036-8075; online ISSN 1095-9203) is published by the American Association for the Advancement of Science, 1200 New York Avenue NW, Washington, DC 20005. The title *Science* is a registered trademark of AAAS.

Science (print ISSN 0036-8075; online ISSN 1095-9203) is published by the American Association for the Advancement of Science, 1200 New York Avenue NW, Washington, DC 20005. The title *Science* is a registered trademark of AAAS.